

Requirements for Functional Models of the Iron Hydrogenase Active Site: D₂/H₂O Exchange Activity in $\{(\mu\text{-SMe})(\mu\text{-pdt})[\text{Fe}(\text{CO})_2(\text{PMe}_3)]_2\}^+[\text{BF}_4^-]$

Irene P. Georgakaki, Matthew L. Miller, and Marcetta Y. Darensbourg*

Department of Chemistry, Texas A&M University, College Station, Texas 77843

Received September 5, 2002

Hydrogen uptake in hydrogenase enzymes can be assayed by H/D exchange reactivity in H₂/D₂O or H₂/D₂/H₂O mixtures. Diiron(II) complexes that serve as structural models for the active site of iron hydrogenase are not active in such isotope scrambling but serve as precursors to Fe^{II}Fe^{II} complexes that are functional models of [Fe]H₂ase. Using the same experimental protocol as used previously for $\{(\mu\text{-H})(\mu\text{-pdt})[\text{Fe}(\text{CO})_2(\text{PMe}_3)]_2\}^+$, **1-H⁺** (Zhao et al. *J. Am. Chem. Soc.* **2001**, *123*, 9710), we now report the results of studies of $\{(\mu\text{-SMe})(\mu\text{-pdt})[\text{Fe}(\text{CO})_2(\text{PMe}_3)]_2\}^+$, **1-SMe⁺**, toward H/D exchange. The **1-SMe⁺** complex can take up H₂ and catalyze the H/D exchange reaction in D₂/H₂O mixtures under photolytic, CO-loss conditions. Unlike **1-H⁺**, it does not catalyze H₂/D₂ scrambling under anhydrous conditions. The molecular structure of **1-SMe⁺** involves an elongated Fe^{II}–Fe separation, 3.11 Å, relative to 2.58 Å in **1-H⁺**. It is proposed that the strong SMe[−] bridging ligand results in catalytic activity localized on a single Fe^{II} center, a scenario that is also a prominent possibility for the enzyme active site. The single requirement is an open site on Fe^{II} available for binding of D₂ (or H₂), followed by deprotonation by the external base H₂O (or D₂O).

Introduction

The connection between enzymes that take up and activate molecular hydrogen and noble metals that show similar functions has intrigued scientists since the discovery of hydrogenases in 1931.¹ The recent wave of attention has been fueled by protein crystal structures which provide striking snapshots of binuclear active sites in both nickel–iron² and iron hydrogenases.³ The similarity of the active site structure

of Fe-only hydrogenase, [Fe]H₂ase, to easily synthesized and well-known dinuclear Fe^IFe^I organometallic complexes⁴ (Figure 1a and b, respectively) has inspired the preparation of derivatives modified in such a way to better mimic the features of the enzyme active site.⁵ Whereas the enzyme is characterized by at least three different oxidation levels, mixed-valent Fe^IFe^{II} is a prominent candidate for the form that is responsible for H₂ uptake; heterolytic (H⁺/H[−]) cleavage; and, by microscopic reversibility, H₂ production and evolution.⁶

* Author to whom correspondence should be addressed. E-mail: marcetta@mail.chem.tamu.edu.

- (1) Stephenson, M.; Stickland, L. H. *Biochem. J.* **1931**, *25*, 205.
- (2) (a) Volbeda, A.; Charon, M.-H.; Piras, C.; Hatchikian, E. C.; Frey, M.; Fontecilla-Camps, J. C. *Nature* **1995**, *373*, 580. (b) Volbeda, A.; Garcin, E.; Piras, C.; De Lacey, A. L.; Fernandez, V. M.; Hatchikian, E. C.; Frey, M.; Fontecilla-Camps, J. C. *J. Am. Chem. Soc.* **1996**, *118*, 12989. (c) Garcin, E.; Vernede, X.; Hatchikian, E. C.; Volbeda, A.; Frey, M.; Fontecilla-Camps, J. C. *Structure* **1999**, *7*, 557. (d) Higuchi, Y.; Yagi, T.; Yasuoka, N. *Structure* **1997**, *5*, 1671. (e) Higuchi, Y.; Ogata, H.; Miki, K.; Yasuoka, N.; Yagi, T. *Structure* **1999**, *7*, 549.
- (3) (a) Peters, J. W.; Lanzilotta, W. N.; Lemon, B. J.; Seefeldt, L. C. *Science* **1998**, *282*, 1853. (b) Nicolet, Y.; Piras, C.; Legrand, P.; Hatchikian, C. E.; Fontecilla-Camps, J. C. *Structure* **1999**, *7*, 13. (c) Nicolet, Y.; De Lacey, A. L.; Vernede, X.; Fernandez, V. M.; Hatchikian, E. C.; Fontecilla-Camps, J. C. *J. Am. Chem. Soc.* **2001**, *123*, 1596. (d) Lemon, B. J.; Peters, J. W. *Biochemistry* **1999**, *38*, 12969.

- (4) Seyferth, D.; Womack, G. B.; Gallagher, M. K.; Cowie, M.; Hames, B. W.; Fackler, J. P., Jr.; Mazany, A. M. *Organometallics* **1987**, *6*, 283.
- (5) (a) Lyon, E. J.; Georgakaki, I. P.; Reibenspies, J. H.; Darensbourg, M. Y. *Angew. Chem., Int. Ed.* **1999**, *38*, 3178. (b) Schmidt, M.; Contakes, S. M.; Rauchfuss, T. B. *J. Am. Chem. Soc.* **1999**, *121*, 9736. (c) Le Cloirec, A.; Best, S. P.; Borg, S.; Davies, S. C.; Evans, D. J.; Hughes, D. L.; Pickett, C. J. *Chem. Commun.* **1999**, 2285. (d) Lawrence, J. D.; Li, H.; Rauchfuss, T. B.; Bénard, M.; Rohmer, M.-M. *Angew. Chem., Int. Ed.* **2001**, *40*, 1768. (e) Razavet, M.; Davies, S. C.; Hughes, D. L.; Pickett, C. J. *Chem. Commun.* **2001**, 847.
- (6) (a) Popescu, C. V.; Münck, E. *J. Am. Chem. Soc.* **1999**, *121*, 7877. (b) Pereira, A. S.; Tavares, P.; Moura, I.; Moura, J. J. G.; Huynh, B. H. *J. Am. Chem. Soc.* **2001**, *123*, 2771. (c) De Lacey, A. L.; Stadler, C.; Cavazza, C.; Hatchikian, E. C.; Fernandez, V. M. *J. Am. Chem. Soc.* **2000**, *122*, 11232. (d) Bennett, B.; Lemon, B. J.; Peters, J. W. *Biochemistry* **2000**, *39*, 7455.

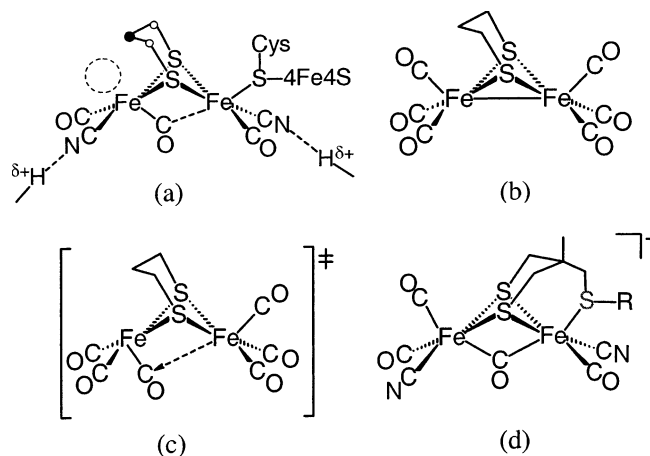


Figure 1. Stick drawing structures of (a) active site of [Fe]H₂ase,³ (b) ground state of (μ-pdt)Fe₂(CO)₆, (c) calculated transition state of Fe(CO)₃ unit rotation in (μ-pdt)Fe₂(CO)₆,⁸ and (d) a spectroscopically observed Fe^{II}-Fe^I complex.⁷

The synthesis of mixed-valent complexes is not easily achieved in the chemist's laboratory. A recent spectroelectrochemical study provided evidence for such an Fe^{II}Fe^I species generated by one-electron oxidation of a diiron(I) model.⁷ The mixed-valent product is a good spectroscopic match for the CO-inhibited oxidized form of the enzyme,^{3d} resulting in the proposed structure shown in Figure 1d. The bridging carbonyl of the Fe^{II}Fe^I complex has not heretofore been observed in (μ-SRS)[Fe^I(CO)₂L]₂ model complexes. Nevertheless, DFT computations suggest an analogous structure as a transition state for a rotation process that equilibrates CO ligands in individual Fe(CO)₃ units as seen in ¹³C NMR spectra. This rotation accounts for the observed fluxionality or intramolecular site exchange that interchanges CO_{apical} with CO_{basal} (Figure 1c).⁸

Although the electrochemically generated Fe^{II}Fe^I species has not, as yet, been isolated, homovalent Fe^{II}Fe^{II} complexes are readily obtained from Fe^IFe^I precursors via the binuclear oxidative addition of electrophiles such as H⁺ or SMe⁺.⁹ Reaction of (μ-pdt)[Fe(CO)₂(PMe₃)₂]₂, complex **1** (pdt = SCH₂CH₂CH₂S), with H⁺ or SMe⁺ produces {(μ-H)(μ-pdt)-[Fe(CO)₂(PMe₃)₂]₂}⁺, **1-H⁺**,¹⁰ or {(μ-SMe)(μ-pdt)[Fe(CO)₂(PMe₃)₂]₂}⁺, **1-SMe⁺**, respectively, with concomitant blue shifts in the ν(CO) IR spectrum (Figure 2). The role of the PMe₃ ligands, analogues to cyanide in the enzyme active site, is to both increase the electron density in the Fe^IFe^I bond and to stabilize the Fe^{II}Fe^{II} oxidation level following oxidative addition.

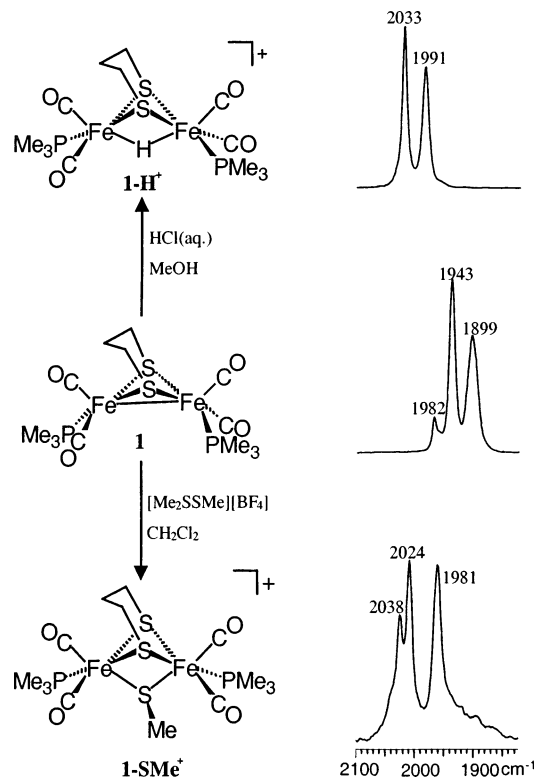
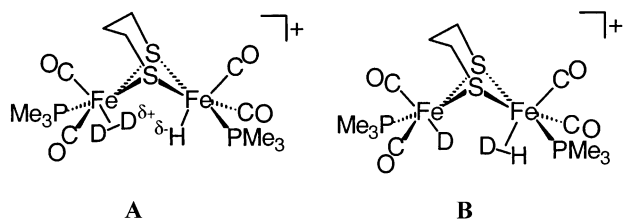


Figure 2. Stick drawing structures and infrared spectra of **1**, **1-H⁺**, and **1-SMe⁺**.

As early as 1934, Farkas, Farkas, and Yudkin demonstrated that hydrogenase from *B. coli* (*Balantidium coli*) catalyzed the isotope exchange reaction between D₂O and H₂.¹¹ This reactivity, together with ortho/para H₂ interconversion, the mechanism of which was studied in detail by Krasna and Rittenberg,¹² has provided the basis for hydrogenase activity assays that typically demonstrate H₂ uptake as indicated by H/D exchange in H₂/D₂O mixtures.¹³ Mixtures of H₂/D₂ have also been reported to show scrambling,¹⁴ presumably via H₂O mediation. On the basis of such test reactions, our previous studies indicated that the diiron(II) complex, **1-H⁺**, serves as a functional model of [Fe]H₂ase in the catalytic isotopic scrambling of D₂/H₂O and H₂/D₂ mixtures.^{10,15} During these processes, all of which require photolysis, **1-H⁺** becomes **1-D⁺**, indicating involvement of the bridging hydride in the isotope exchange mechanism. Intermediates such as structures **A** and **B**, call upon the μ-H to shift to a terminal position and serve as an internal base under anhydrous conditions to deprotonate the proximate (η²-H₂)Fe^{II} moiety. A weak external base such as H₂O can also deprotonate the acidic (η²-H₂)Fe^{II} intermediate.¹⁶

- (7) Razavet, M.; Borg, S. J.; George, S. J.; Best, S. P.; Fairhurst, S. A.; Pickett, C. J. *Chem. Commun.* **2002**, 700.
 (8) (a) Georgakaki, I. P.; Thomson, L. M.; Lyon, E. J.; Hall, M. B.; Darensbourg, M. Y. *Coord. Chem. Rev.*, manuscript submitted. (b) Lyon, E. J.; Georgakaki, I. P.; Reibenspies, J. H.; Darensbourg, M. Y. *J. Am. Chem. Soc.* **2001**, *123*, 3268.
 (9) (a) Fauvel, K.; Mathieu, R.; Poiblanc, R. *Inorg. Chem.* **1976**, *15*, 976. (b) Savariault, J.-M.; Bonnet, J.-J.; Mathieu, R.; Galy, J. C. *R. Acad. Sci.* **1977**, *284*, C663. (c) Lyons, L. J.; Anderson, L. L.; Crane, R. A.; Treichel, P. M. *Organometallics* **1991**, *10*, 587. (d) Treichel, P. M.; Crane, R. A.; Matthews, R.; Bonnin, K. R.; Powell, D. J. *Organomet. Chem.* **1991**, *402*, 233.
 (10) Zhao, X.; Georgakaki, I. P.; Miller, M. L.; Yarbrough, J. C.; Darensbourg, M. Y. *J. Am. Chem. Soc.* **2001**, *123*, 9710.

- (11) Farkas, A.; Farkas, L.; Yudkin, J. *Proc. R. Soc. (London)* **1934**, *B115*, 373.
 (12) Krasna, A. I.; Rittenberg, D. *J. Am. Chem. Soc.* **1954**, *76*, 3015.
 (13) (a) Adams, M. W. W.; Mortenson, L. E.; Chen, J.-S. *Biochim. Biophys. Acta* **1981**, *594*, 105. (b) Albracht, S. P. J. *Biochim. Biophys. Acta* **1994**, *1188*, 167.
 (14) Yagi, T. *J. Biochem.* **1970**, *68*, 649.
 (15) Zhao, X.; Georgakaki, I. P.; Miller, M. L.; Mejia-Rodriguez, R.; Chiang, C.-Y.; Darensbourg, M. Y. *Inorg. Chem.* **2002**, *41*, 3917.
 (16) Landau, S. E.; Morris, R. H.; Lough, A. J. *Inorg. Chem.* **1999**, *38*, 6060.



Because an open site on Fe can, under photolysis, be created by a hydride shift or by CO loss, we questioned whether the hydride was a requirement for the heterolytic $\text{H}_2/\text{H}_2\text{O}$ or $\text{D}_2/\text{H}_2\text{O}$ cleavage reaction. Hence, the following study was designed to assess the requirement of a H^- ligand in candidates for H_2 ase functional models.

Experimental Section

Materials and Techniques. All manipulations were performed using standard Schlenk-line and syringe/rubber-septa techniques under N_2 or in an argon atmosphere glovebox. Solvents were of reagent grade and purified as follows: Dichloromethane was distilled over P_2O_5 under N_2 . Acetonitrile was distilled once from CaH_2 , distilled once from P_2O_5 , and freshly distilled from CaH_2 immediately before use. Diethyl ether was distilled from sodium/benzophenone under N_2 . The following materials were of reagent grade and used as received: $\text{Fe}_3(\text{CO})_{12}$, 1,3-propanedithiol, MeSSMe , Me_3OBF_4 and NH_4PF_6 (Aldrich Chemical Co.); deuterated solvents and D_2 (Cambridge Isotope Laboratories).

Infrared spectra were recorded on a Mattson 6021 FTIR spectrometer with DTGS and MCT detectors. ^1H , ^{13}C , and ^{31}P NMR (85% H_3PO_4 was used as an external reference) spectra were recorded on a Unity+ 300-MHz superconducting NMR instrument operating at 299.9, 75.43, and 121.43 MHz, respectively. ^2H NMR spectra were recorded on a Unity Inova-400 NMR instrument with a 5-mm autoswitchable probe operating at 61.35 MHz and on a VXR-300 NMR instrument operating at 46.05 MHz.

Preparations. The neutral dinuclear iron compounds were prepared according to literature procedures.¹⁵

$[\text{Me}_2\text{SSMe}^+][\text{BF}_4^-]$. Following the published procedure,¹⁷ a solution containing 0.74 mL of methyl disulfide (8.06 mmol) in ~ 7 mL of CH_3CN was added dropwise to an equimolar amount of $\text{Me}_3\text{O}^+\text{BF}_4^-$ (1.04 g, 8.06 mmol) dissolved in ~ 8 mL of CH_3CN at 0°C . After the mixture had been stirred for ~ 2 h at 0°C , dry ether was added to precipitate dimethylthiomethylsulfonium fluoroborate ($[\text{Me}_2\text{SSMe}^+][\text{BF}_4^-]$) as a white solid that was stored in the glovebox at -36°C (1.1 g; yield, 69%).

Synthesis of $\{(\mu\text{-SMe})(\mu\text{-pdt})[\text{Fe}(\text{CO})_2(\text{PMe}_3)]_2\}^+[\text{BF}_4^-]$. A red solution of 0.97 g of $(\mu\text{-pdt})[\text{Fe}(\text{CO})_2(\text{PMe}_3)]_2$ (2 mmol) in ~ 50 mL of dry CH_2Cl_2 was transferred via cannula into a Schlenk flask containing 0.41 g (2 mmol) of $[\text{Me}_2\text{SSMe}^+][\text{BF}_4^-]$. Following overnight stirring at 22°C , the IR spectrum [$\nu(\text{CO})$ region] showed the presence of a mixture of the neutral precursor and the cationic product in the brown solution. After the mixture had been filtered through Celite under Ar and concentrated in a vacuum, dry Et_2O was added to precipitate the product and remove the unreacted neutral complex, **1**. Crystals suitable for an X-ray crystal structure determination were grown from CH_2Cl_2 solutions layered with Et_2O at -5°C . Infrared spectrum, $\nu(\text{CO})$, CH_2Cl_2 : 2038(m), 2024(s), 1981(s) cm^{-1} . Because of the difficulty in isolating the product in the solid form as its BF_4^- salt, the PF_6^- salt was prepared by ion exchange reaction of $\{(\mu\text{-SMe})(\mu\text{-pdt})[\text{Fe}(\text{CO})_2(\text{PMe}_3)]_2\}^+[\text{BF}_4^-]$

(17) Smallcombe, S. H.; Caserio, M. C. *J. Am. Chem. Soc.* **1971**, *93*, 5826.

with saturated aqueous solution of NH_4PF_6 in MeOH. The solid was collected, washed with H_2O and Et_2O , and dried in air (0.6 g; yield, 44%). ^{31}P NMR, acetone- d_6 : 20.95 (PMe_3) and -142.7 ppm (PF_6^-). Elemental analysis, calculated for $\text{Fe}_2\text{C}_{14}\text{H}_{27}\text{S}_3\text{O}_4\text{P}_3\text{F}_6$ (found%): C, 24.92 (24.66); H, 4.00 (4.03).

Test for Catalytic Formation of HD in H_2/D_2 Mixture. A medium-pressure NMR tube (Wilma, 528-PV-7) was charged with a solution containing 20 mg of $\{(\mu\text{-SMe})(\mu\text{-pdt})[\text{Fe}(\text{CO})_2(\text{PMe}_3)]_2\}^+[\text{PF}_6^-]$ in 1 g of CD_2Cl_2 . The tube was then pressurized with 5 bar H_2 and with D_2 to a total pressure of 10 bar and exposed to sunlight. ^1H NMR spectra were taken daily over the course of 8 days to check the formation of HD. None was observed.

H/D Exchange in $\text{D}_2/\text{H}_2\text{O}$ Mixture. A 0.8-mL portion of a solution made from 0.15 g of $[\mathbf{1}\text{-SMe}^+][\text{PF}_6^-]$ in 3 mL of CH_2Cl_2 was put in a medium-pressure NMR tube together with 2 μL of H_2O . The tube was pressurized with 10 bar D_2 and exposed to sunlight. ^2H NMR spectra were taken at time intervals to follow the formation of HOD.

^{13}C CO Exchange Experiment in $[(\mu\text{-SMe})(\mu\text{-pdt})(\text{Fe}(\text{CO})_2\text{-PMe}_3)_2]^+[\text{PF}_6^-]$. A 0.7-mL portion of a solution made from 23 mg of $[\mathbf{1}\text{-SMe}^+][\text{PF}_6^-]$ in 1.6 mL of d_6 -acetone was transferred into a medium-pressure NMR tube. The tube was lightly degassed, filled with 20 psi ^{13}CO , and exposed to sunlight. The ^{13}C NMR spectrum after 1 day showed two doublets (208.95 and 208.07 ppm, $J_{\text{C-P}} = 19.5$ and 14.6 Hz, respectively) in the CO region, indicating the incorporation of ^{13}CO into the complex. The $\nu(\text{CO})$ infrared spectrum in CH_2Cl_2 showed a shift of the stretching frequencies to lower wavenumbers consistent with $^{13}\text{CO}/^{12}\text{CO}$ exchange in $\mathbf{1}\text{-SMe}^+$. Infrared spectrum, $\nu(\text{CO})$ region: $\nu(\text{CO})$, $\mathbf{1}\text{-SMe}^+$ 2038, 2024, 1981; $\nu(\text{CO})$, ^{13}CO -enriched $\mathbf{1}\text{-SMe}^+$ 2020, 1981, 1947 cm^{-1} .

X-ray Structure Determination. A single crystal was mounted on a glass fiber at 110 K. The X-ray data were collected on a Bruker Smart 1000 CCD diffractometer and covered a hemisphere of reciprocal space by a combination of three sets of exposures. The space group was determined on the basis of systematic absences and intensity statistics. Crystal data for $[\mathbf{1}\text{-SMe}^+][\text{BF}_4^-]$: $\text{C}_{14}\text{H}_{27}\text{O}_4\text{P}_2\text{S}_3\text{BF}_4\text{Fe}_2$, $M = 616.01$, orthorhombic, space group $Pnma$, $a = 14.79(3)$ Å, $b = 12.54(2)$ Å, $c = 12.98(2)$ Å, $\alpha = 90^\circ$, $\beta = 90^\circ$, $\gamma = 90^\circ$, $V = 2408(7)$ Å³, $Z = 4$, $D_c = 1.699$ g cm^{-3} . The structure was solved by direct methods. Hydrogen atoms were placed at idealized positions and refined with fixed isotropic displacement parameters. The pdt bridge was refined with “envelope-flap” disorder. Anisotropic refinement for all non-hydrogen atoms was done by a full-matrix least-squares method with $R1 = 0.0592$ and $wR2 = 0.0956$. Programs used include SMART¹⁸ for data collection and cell refinement, SAINTPLUS¹⁹ for data reduction, SHELXS-86 (Sheldrick)²⁰ for structure solution, SHELXL-97 (Sheldrick)²¹ for structure refinement, and SHELXTL-Plus, version 5.1 or later (Bruker),²² for molecular graphics and preparation of material for publication.

Results and Discussion

Reaction of $(\mu\text{-pdt})[\text{Fe}(\text{CO})_2(\text{PMe}_3)]_2$, **1**, with the SMe^+ synthon, $[\text{Me}_2\text{SSMe}^+][\text{BF}_4^-]$, in CH_2Cl_2 results in the

(18) SMART 1000 CCD; Bruker Analytical X-ray Systems: Madison, WI, 1999.

(19) SAINT-Plus, version 6.02; Bruker: Madison, WI, 1999.

(20) Sheldrick, G. SHELXS-86: Program for Crystal Structure Solution; Institut für Anorganische Chemie, Universität Göttingen: Göttingen, Germany, 1986.

(21) Sheldrick, G. SHELXL-97: Program for Crystal Structure Refinement; Institut für Anorganische Chemie, Universität Göttingen: Göttingen, Germany, 1997.

(22) SHELXTL, version 5.1 or later; Bruker: Madison, WI, 1998.

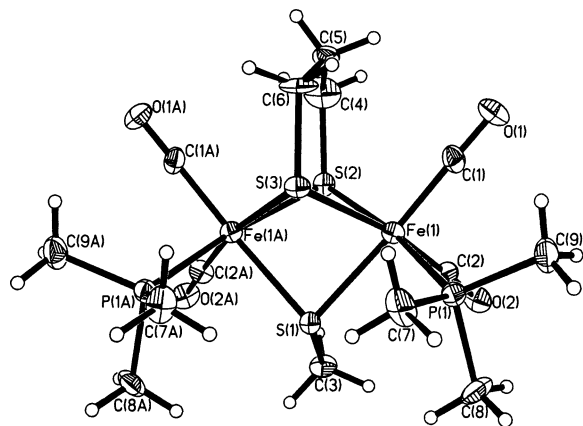


Figure 3. Thermal ellipsoid representation (30% probability) of the molecular structure of **1-SMe⁺**.

Table 1. Selected Metric Data for **1**, **1-H⁺**, and **1-SMe⁺**

	1	1-H⁺	1-SMe⁺
Fe···Fe	2.555(2)	2.5784(8)	3.109
S···S	3.026	3.064	2.976
Fe–P	2.234(3)	2.2523(12)	2.257(4)
Fe–CO _{ap}	1.772(9)	1.779(4)	1.774(11)
Fe–CO _{ba}	1.742(10)	1.778(4)	1.764(10)
Fe–S(pdt-br) ^a	2.254(2)	2.2717(11)	2.324(4)
Fe–SMe	N/A	N/A	2.304(4)
Fe–S–Fe ^a	69.06(8)	69.15(4)	84.0(2)
S–Fe–S ^a	84.34(11)	84.77(4)	79.50(14)
Fe dsp ^b	0.376	0.231	0.153

^a Average of all equivalent bonds and angles. ^b Fe dsp = average displacement of the Fe atoms out of the best planes defined by the two S's of the pdt bridge, C of basal CO, and P atoms.

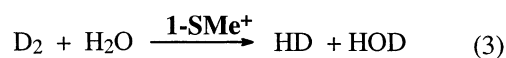
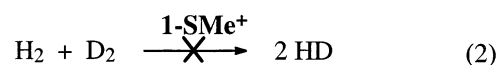
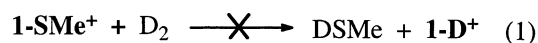
formation of $\{(\mu\text{-SMe})(\mu\text{-pdt})[\text{Fe}(\text{CO})_2(\text{PMe}_3)_2]^+\}[\text{BF}_4^-]$, **1-SMe⁺**. Crystals of **[1-SMe⁺][BF₄⁻]** suitable for X-ray structure determination were grown in CH₂Cl₂ solution layered with Et₂O at –5 °C. The descriptions of **1-SMe⁺**, as a stick drawing Figure 2 and a thermal ellipsoid plot in Figure 3, display the molecular structure as a biotetrahedron, face-bridged by three thiolates.

For the neutral precursor **1** and other $(\mu\text{-SRS})[\text{Fe}^{\text{I}}(\text{CO})_2\text{L}]_2$ complexes, which are described as edge-bridged bisquare pyramids, the positions of the L ligands are defined as apical, basal, cisoid, and transoid. Although the oxidative addition products **1-H⁺** and **1-SMe⁺** are face-bridged biotetrahedra, we have retained the designations for the L positions from the neutral precursor. As defined by crystallography, the repositioning of the PMe₃ ligands from the basal/basal transoid conformation in **1** and **1-H⁺**¹⁰ to basal/basal cisoid in **1-SMe⁺** minimizes steric interactions of the PMe₃ ligands with the SMe bridge. The shift in the $\nu(\text{CO})$ IR spectral values as **1** is converted to **1-SMe⁺** is similar to that for **1-H⁺**, i.e., approximately +70 cm⁻¹ (Figure 2). The change in pattern, i.e., the splitting of the high-frequency band into two, is evidence of the change in symmetry described above.

Key structural metric data for **1**, **1-H⁺**, and **1-SMe⁺** are listed in Table 1. The dramatic increase in the Fe···Fe distance of ca. 0.5 Å with the four-electron donor SMe⁻ as the bridge has several consequences. The average of the Fe–S–Fe angle increases to 84.0(2)° in **1-SMe⁺**, from the average of 69° in the parent **1** and **1-H⁺**, resulting in a

flattening of the Fe₂(pdt-S)₂ core without significant change in the S···S cross-ring distance. The FeS₂C₃ metallocyclohexane rings are maintained in the typical chair/boat configuration with normal distances. An additional consequence of the four-electron-donor $\mu\text{-SMe}^-$ vs the two-electron-donor $\mu\text{-H}^-$ bridge is the increased octahedral character of the FeS₃(CO)₂PMe₃ coordination spheres. As measured by the displacement of the Fe from the (pdt-S₂)-(CO)(P) plane, the value is ~0.38 Å in complex **1**, which has the two electrons of the Fe–Fe bond in the sixth coordination position; it decreases to 0.23 Å in **1-H⁺** and decreases further in **1-SMe⁺** to 0.15 Å.

Activity of 1-SMe⁺ as an H/D Exchange Catalyst. Reactivity studies of **1-SMe⁺** were based on the experimental protocol used to explore the H₂ activation and H/D exchange capabilities of **1-H⁺** and analogues.^{10,15} To establish whether the $\mu\text{-SMe}$ moiety might exchange with D⁻ derived from D₂, a medium-pressure NMR tube containing **[1-SMe⁺][PF₆⁻]** in CH₂Cl₂ was pressurized with 10 bar D₂ and exposed to sunlight as described in the Experimental Section. The ²H NMR monitor found no $(\mu\text{-D})\text{Fe}_2^+$ or MeSD formed (eq 1). In the same time period, significant amounts of H/D exchange was observed for **1-H⁺**/D₂ mixtures.^{10,15} Similarly to the experiment with **1-H⁺**, H₂/D₂ gaseous mixtures were introduced into an anhydrous CD₂Cl₂ solution of **1-SMe⁺**. In the absence of light, as well as with extended periods of photolysis (sunlight for 8 days or more), no HD was observed in the ¹H NMR spectrum (eq 2). Under the same conditions, **1-H⁺** showed extensive scrambling of isotopes (formation of HD from H₂ and D₂ as well as formation of **1-D⁺**).^{10,15}



In contrast, mixtures of D₂ and H₂O show substantial H/D exchange with both **1-SMe⁺** and **1-H⁺** as catalysts (eq 3). A sample containing **1-SMe⁺** and 2 μL of H₂O in CH₂Cl₂ was pressurized with 10 bar D₂ and exposed to sunlight. To follow the formation of HOD, ²H NMR spectra were recorded after 1, 2, and 4 h of exposure (Figure 4). After 1 h of photolysis, the spectrum showed a resonance at 1.75 ppm corresponding to the dissolved D-enriched water. Its intensity was 0.75 relative to the natural-abundance deuterium in the solvent, CH₂Cl₂, which appears at 5.32 ppm. Within 4 h of exposure to sunlight, this resonance shifted slightly to 1.80 ppm, and its intensity increased to 8.53 times that of the solvent peak, indicating significant exchange between D₂ and H₂O in the presence of **1-SMe⁺**.

Conclusions

The conclusions and mechanistic implications of the above study are summarized as follows. The biotetrahedral Fe^{II}Fe^{II} complex, **1-SMe⁺**, face-bridged by three thiolates, $(\mu\text{-SMe})$ -

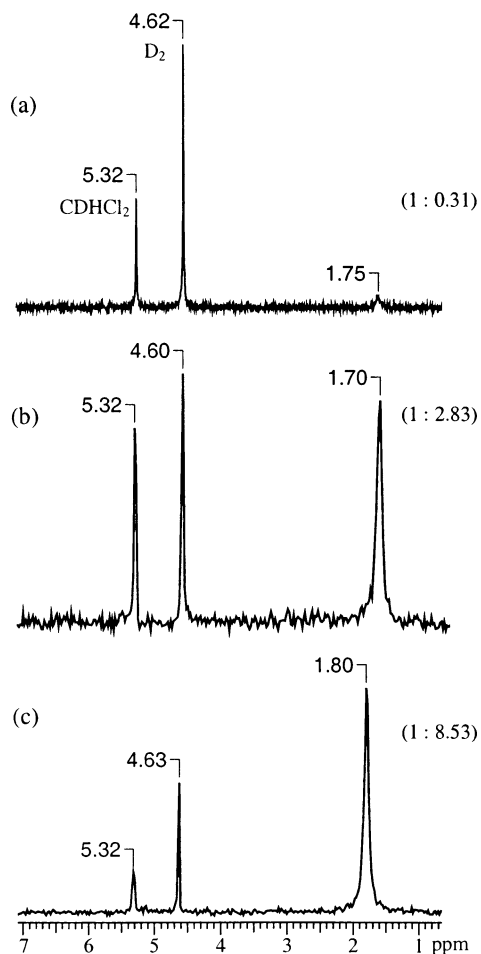
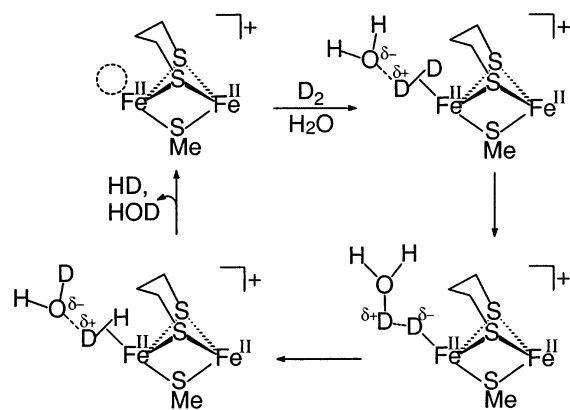


Figure 4. ^2H NMR spectra showing the formation of HOD ($\delta = 1.70$ – 1.80 ppm) in a CH_2Cl_2 solution containing **1-SMe** $^+$ as the PF_6^- salt, 10 bar D_2 , and $2\ \mu\text{L}$ of H_2O : (a) before exposure to sunlight, (b) after 2 h of photolysis, and (c) after 4 h of photolysis. Relative ratio of (natural abundance, $\delta = 5.32$ ppm) CH_2Cl_2 and HOD in parentheses.

(μ -pdt), maintains the H/D exchange capability in $\text{D}_2/\text{H}_2\text{O}$ mixtures that was detected for the analogous complex **1-H** $^+$, face-bridged by a hydride and two thiolates. However, **1-SMe** $^+$ loses the capability for catalysis of H/D exchange in H_2/D_2 mixtures in anhydrous solution as was demonstrated for **1-H** $^+$.^{10,15} Our mechanistic proposal for the latter called upon an open site created by H^- shift or CO loss, as discussed earlier, and deprotonation of ($\eta^2\text{-H}_2$)- Fe^{II} by the internal H^- base. Whether the $\eta^2\text{-H}_2$ and the terminal Fe-H exist on the same Fe^{II} or on adjacent atoms (binuclear activation) depends on whether a CO loss event is concomitant with $\mu\text{-H} \rightarrow \text{t-H}$ conversion. However, such bridge breakage is either excluded or nonproductive in the case of **1-SMe** $^+$, as conversion of $\mu\text{-SMe}$ to $\mu\text{-H}$ was not observed when **1-SMe** $^+$ was pressurized with H_2 . This is consistent with the fact that $\mu\text{-SMe}^-$ is a stronger bridging ligand than $\mu\text{-H}^-$, suggesting that the open site needed for H_2 binding in **1-SMe** $^+$ comes from CO loss. Furthermore the elongated $\text{Fe}\cdots\text{Fe}$ distance of $\sim 3.1\ \text{\AA}$ in **1-SMe** $^+$ relative to $2.6\ \text{\AA}$ in **1-H** $^+$ would prevent involvement of both metals in the H_2 activation process. The rigidity of the bidentate chelating propanedithiolate bridge is expected to prohibit further elongation of the $\text{Fe}\cdots\text{Fe}$ distance and flattening of the butterfly Fe_2S_2 core to a diamond shape, as seen in $\text{L}_4\text{Fe}^{\text{II}}(\mu$ -

Scheme 1



$\text{SR})_2\text{Fe}^{\text{II}}\text{L}_4$ complexes, where the $\text{Fe}^{\text{II}}\cdots\text{Fe}^{\text{II}}$ distance expands to $\sim 3.5\ \text{\AA}$.²³

For both **1-H** $^+$ and **1-SMe** $^+$, an open site is required, as indicated by the need of photolysis for H_2 activation by the external base, H_2O . The creation of an open site in these complexes is consistent with the lability of the CO's indicated by $^{13}\text{CO}/\text{CO}$ exchange under photolysis by sunlight for both **1-H** $^+$ and **1-SMe** $^+$. A compatible mechanism is presented in Scheme 1, where the open site is depicted trans to the $\mu\text{-SMe}$, in analogy with the open site in the H_2ase binuclear active site. Formation of the ($\eta^2\text{-H}_2$)- Fe^{II} interaction is well-precedented, as is the enhanced acidity of the metal-bound H_2 .¹⁶

Thus, the two binuclear model complexes **1-H** $^+$ and **1-SMe** $^+$ mimic the H/D exchange activity of the $[\text{Fe}]_2\text{H}_2\text{ase}$ enzyme in that both demonstrate H_2 (or D_2) uptake and heterolytic cleavage by D_2O (or H_2O) under photolytic conditions. The singular requirement for these processes is an open site on an Fe^{II} center. A built-in hydride is not needed for H/D exchange reactivity in $\text{D}_2/\text{H}_2\text{O}$ or in H_2/D_2 mixtures in the presence of water; it is needed for anhydrous conditions where the mechanism of H_2 activation calls upon cooperation between the two metal sites in true binuclearity. We propose that the **1-SMe** $^+$ model localizes reactivity on one Fe center and engages the second iron only for thiolate ligand modification, maintaining the low-spin Fe^{II} , d^6 configuration conducive to $\eta^2\text{-H}_2$ binding. Thus, the reactivity scenario and structural design that is reasonable for the enzyme active site is an attractive archetype for the mechanism for the model complexes.

Both $[\text{Fe}]_2\text{H}_2\text{ase}$ and $[\text{NiFe}]_2\text{H}_2\text{ase}$ appear to have been designed, protein engineered, to have an open site on iron in their catalytic active sites. Whether both classes of metalloenzymes follow the same mechanism of H_2 uptake on Fe^{II} and cleavage or H_2 formation and evolution from an ($\eta^2\text{-H}_2$)- Fe^{II} species is not at all clear. Convincing experiments by Sellmann, Geipel, and Moll²⁴ demonstrated the possibility of D_2 activation at a nickel(II) thiolate under anhydrous conditions, resulting in D^+/D^- cleavage and formation of Ni-D and nickel-bound RSD in a mononuclear nickel

(23) Liaw, W.-F.; Lee, N.-H.; Chen, C.-H.; Lee, C.-M.; Lee, G.-H.; Peng, S.-M. *J. Am. Chem. Soc.* **2000**, *122*, 488.

(24) Sellmann, D.; Geipel, F.; Moll, M. *Angew. Chem., Int. Ed.* **2000**, *39*, 561.

complex. Would an adjacent Fe^{II} center positioned to trap and hold H₂ in close proximity to Ni–SR enhance this activity? Such a reaction scenario, first expressed by Fontecilla-Camps and co-workers,^{3c} is an attractive possibility in the enzyme active site.

Acknowledgment. We acknowledge financial support from the National Science Foundation (Grants CHE-9812355, CHE-0111629, and CHE 85-13273 for the X-ray

diffractometer and crystallographic computing system) and contributions from the R. A. Welch Foundation. We also thank Dr. Joseph Reibenspies for his assistance in the X-ray crystal structure analysis.

Supporting Information Available: Molecular structure and X-ray crystallographic tables for **1-SMe⁺**. This material is available free of charge via the Internet at <http://pubs.acs.org>.

IC026005+